Extended Depth-of-Field 3-D Display and Visualization by Combination of Amplitude-Modulated Microlenses and Deconvolution Tools

Raul Martínez-Cuenca, Genaro Saavedra, Manuel Martínez-Corral, and Bahram Javidi, *Fellow, IEEE*

***Abstract*—One of the main challenges in 3-D display and visualization is to overcome its limited depth of field. Such limitation is due to the fast deterioration of lateral resolution for out-of-focus object positions. Here we propose a new method to significantly extend the depth of field. The method is based on the combined benefits of a proper amplitude modulation of the microlenses, and the application of deconvolution tools. Numerical tests are presented to verify the theoretical analysis.**

***Index Terms*—Image reconstruction-restoration, resolution, three-dimensional (3-D) image acquisition, 3-D display, 3-D imaging.**

I. Introduction

INTEGRAL IMAGING (InI) is a three-dimensional (3-D) display and visualization technique [1]–[16]. An InI system consists of two consecutive stages. In the image capture (pickup) stage, an array of microlenses generates, onto a sensor such as a charge-coupled device (CCD), a collection of plane elemental images. Each elemental image has a different perspective of the 3-D object. Therefore, the CCD records a set of projections of the object. In contrast to holography, it can operate with incoherent illumination. The capture stage is a passive sensor and it does not require active illumination. In the reconstruction stage, the recorded images are displayed by an optical device, such as a LCD monitor, placed in front of another microlens array. This setup provides the observer with a reconstructed 3-D image with full parallax. InI principles were first proposed by Lippmann [1], and some relevant work was done in the meantime [2]–[6]. The interest in InI was resurrected recently because of its application to 3-D TV and display [7]. It provides autostereoscopic images without the help of any special glasses.

Manuscript received May 31, 2005; revised August 15, 2005. This work was supported in part by the Plan Nacional I + D + I under Grant DPI2003-4698, Ministerio de Ciencia y Tecnología, Spain, and by the Generalitat Valenciana under Grant GV04B-186. The work of R. Martínez-Cuenca was supported by the Universitat de València (Cinc Segles grant).

R. Martinez-Cuenca, G. Saavedra, and M. Martinez-Corral are with the Department of Optics, University of Valencia, E-46100 Burjassot, Spain (e-mail: Manuel.Martinez@uv.es).

B. Javidi is with the Electrical and Computer Engineering Department, University of Connecticut, Storrs, CT 06267-1157 USA (e-mail: bahram@engr.uconn.edu).

Digital Object Identifier 10.1109/JDT.2005.858883

Since its rebirth, InI has overcome many of its challenges. It is remarkable, for example, that a very smart technique for the pseudoscopic to orthoscopic conversion was developed [8]. Some methods were proposed to overcome the limits in lateral resolution imposed by the pixelated structure of the CCD [9]–[11], or by the microlens array [12], [13]. Another challenge faced is the enhancement of the depth of field (DOF) [14], [15]. It sounds, however, slightly surprising at this point that, to our knowledge, the use of deconvolution tools to improve the quality of recorded images has still not been proposed. In fact, there is a reason for that, as we explain next.

Since an InI system forms a 2-D image of a 3-D scene at any elemental cell, only some parts of the 3-D scene belong to the in-focus plane, and therefore they produce onto the cell the corresponding Airy disk. On the contrary, the out-of-focus points produce a blurred version of the Airy disk. Since we deal with 3-D surface objects, some parts of the object produce a blurred image. Then, the response of the system to points of different lateral (and therefore axial) coordinates is different [16]. In other words, InI systems are not linear and shift invariant (LSI). Consequently, in InI neither a point-spread function (PSF), nor an optical transfer function (OTF) can be defined. Therefore, to remedy out of focus problems [17] deconvolution tools [18]–[20] could not be properly applied in principle to these kinds of systems.

What we propose here is a way to overcome this problem. We propose first the binary amplitude modulation of the capture microlenses. Such modulation has shown to be a very effective way to increment the DOF of InI systems. This is because the amplitude modulation allows the impulse response to degrade very slowly for out-of-focus positions. Thus, now it is possible to define in good approximation an effective PSF over a wide range of out-of-focus positions. Consequently, deconvolution tools can now be used to improve the quality of the elemental images. The proposed method has many benefits in 3-D TV, 3-D display, and 3-D visualization [21], [22].

The paper is organized as follows. Section II is devoted to a review of the principles of InI pickup for 3-D image pick-up and display. In Section III, we show that the binary amplitude modulation permits to define an effective PSF over a wide range of axial positions. In Section IV we review the principles of deconvolution Wiener filtering, and we calculate its parameters

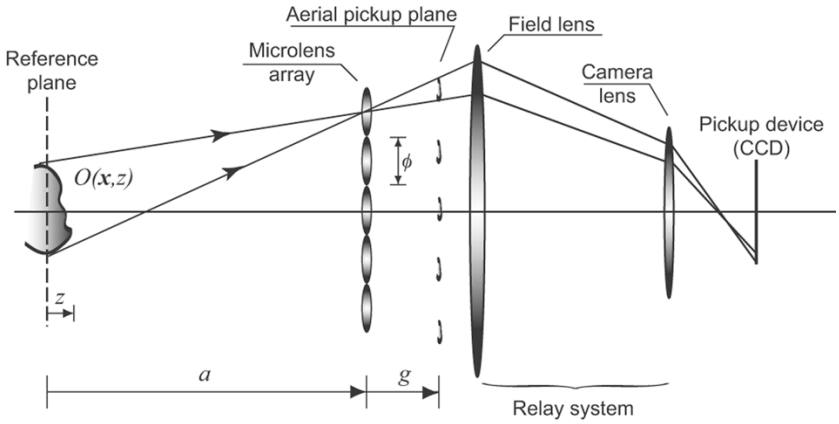

Fig. 1. Scheme, not to scale, of the capture setup of a 3-D integral imaging system. Points of the surface object, $O(\mathrm{x},\mathrm{z})$, out of reference plane produce blurred images in the aerial pickup plane. In the relay system the field lens collects the rays proceeding from the outermost microlenses whereas the camera lens projects the images onto the CCD.

to perform an optimum, automatic deconvolution in InI. Finally, in Section V we outline the main achievements of this work.

II. The 3-D Image Pick-Up Stage

Consider the capture setup of an InI system. As shown in Fig. 1, a 3-D surface object is illuminated by a spatially-incoherent light beam of mean wavelength λ. The light emitted by the surface object is collected by the microlens array to form a collection of 2-D elemental aerial images. The reference and the aerial pickup planes are conjugated through the microlenses so that distances a and g are related by the lens law $1/a + 1/g = 1/f$. A relay system projects the aerial images into the pickup device (CCD). The lateral magnification of the relay system is adjusted so that the size of the elemental-images collection matches the CCD size.

Since incoherent illumination is assumed, the intensity distribution of light scattered by the surface object can be represented by

$$O(\mathbf{x}, z) = R(\mathbf{x})\delta(z - f(\mathbf{x})) \tag{1}$$

where the function $R(\mathbf{x})$ accounts for the object's intensity reflectivity and $f(\mathbf{x}) - z = 0$ is the function that describes the surface. In a previous paper [16] we demonstrated that the intensity distribution corresponding to the elemental image provided by the microlens of index $\mathbf{m} = (m, n)$ is given by

$$I_\lambda^{\mathbf{m}}(\mathbf{x}') = \int_{\Sigma_O} R(\mathbf{x}) H_\lambda^{\mathbf{m}}(\mathbf{x}' - M_z\mathbf{x}; z = f(\mathbf{x}))d^2\mathbf{x} \tag{2}$$

where Σ_O is the surface of the object and

$$H_\lambda^{\mathbf{m}}(\mathbf{x}' - M_z\mathbf{x}; z) \equiv \left|\tilde{\mathrm{P}}_z\left(\frac{\mathbf{x}' - M_z\mathbf{x}}{\lambda g}\right)\right|^2 \otimes \delta(\mathbf{x}' - \mathbf{m}p(1 - M_z)) \tag{3}$$

is the intensity at a given point $\mathbf{x}' = (x', y')$ of the aerial pickup plane produced by an arbitrary point $(\mathbf{x}, z)$ on the surface object. Here $\delta(\bullet)$ is the Dirac delta function, $\otimes$ denotes the 2-D convolution product, and $\tilde{\mathrm{P}}_z$ stands for the 2-D Fourier transform of the generalized pupil function.

$$\mathrm{P}_z(\mathbf{x_o}) = p(\mathbf{x_o}) \exp\left\{i\frac{\pi}{\lambda}\left(\frac{1}{a - z} - \frac{1}{a}\right)|\mathbf{x_o}|^2\right\} \tag{4}$$

where $p(\mathbf{x_o})$ accounts for the pupil function of the microlenses. Clearly, p stands for the constant pitch of the microlens array and $M_z = -g/(a - z)$ is a magnification factor that depends on the depth coordinate z.

An important outcome from (2) is that the system is not 2-D linear and shift invariant (LSI). This is because the impulse response $H_\lambda^{\mathbf{m}}$ strongly depends on the depth coordinate, and consequently on the value of the lateral coordinate. Thus, the PSF of the system cannot be rigorously defined.

Additionally, in real image acquisition tasks the presence of additive noise degrades the quality of recorded images. In particular, the use of CCDs as capturing devices leads to the addition of three types of noise. The so-called CCD noise summarizes all the noise sources due to the image sensor, such as dark current, transfer noise, fixed pattern noise, reset noise and on-chip amplifier noise. The readout noise is caused by off-chip amplification and analog-to-digital conversion. Finally, the shot noise appears due to the statistical nature of the photodetection process. Since these noise types are uncorrelated, the noise power is given by

$$n_{\mathrm{All}} = \sqrt{n_{\mathrm{CCD}}^2 + n_{\mathrm{READOUT}}^2 + n_{\mathrm{SHOT}}^2}. \tag{5}$$

However, the shot noise is dominant when the illumination intensity exceeds 0.1 mW/m^2. If the typical working intensity range in InI is over this limit, the recorded elemental images are accurately described

$$\mathrm{I}_\lambda^{\mathbf{m}}(\mathbf{x}') = I_\lambda^{\mathbf{m}}(\mathbf{x}') + n_{\mathrm{SHOT}}^{\mathbf{m}}(\mathbf{x}'). \tag{6}$$

III. Binary Amplitude Modulation

As stated above, one of the main challenges of InI is its limited DOF. To illustrate this limitation, we have performed a numerical experiment in which we obtain the elemental images of a computer-synthesized object that is axially displaced. Since

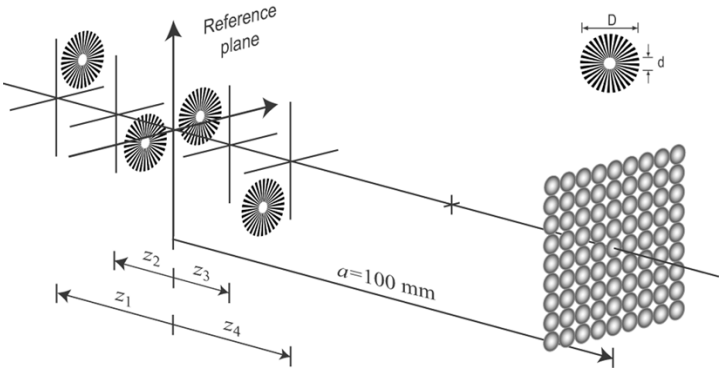

Fig. 2. Scheme, not to scale, of the integral imaging numerical experiment. The inner and outer diameters of the spoke target used in our experiments were $d = 0.4$ and $D = 2.0$ mm, respectively.

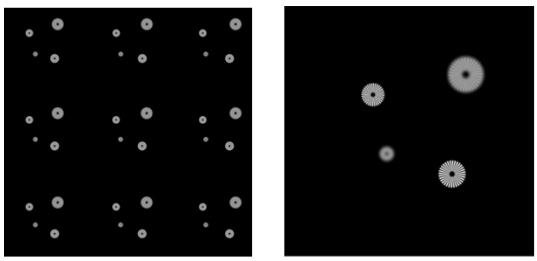

Fig. 3. (a) 2-D elemental images of the spoke targets captured from nine different views. (b) Enlarged view of the central elemental image.

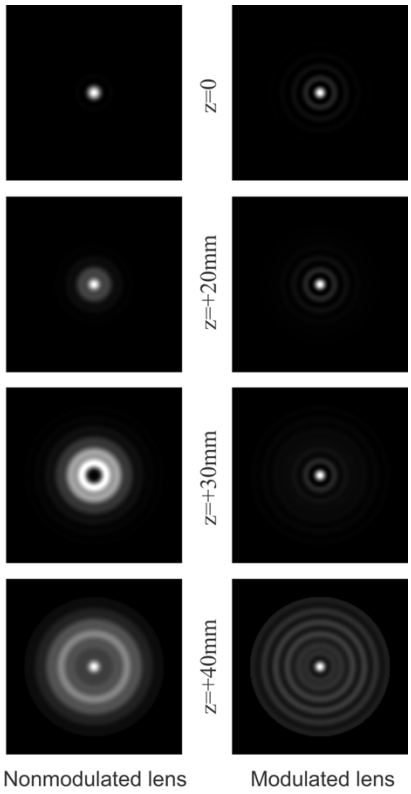

Fig. 4. Cross sections of function $H_\lambda^0(\mathbf{x}, z)$ corresponding to the nonmodulated lenses and the amplitude-modulated lenses. The filters consist in an opaque circular mask of diameter $\delta\phi$ (with $\delta = 1/\sqrt{2}$) centered just behind each microlens.

the aim of the numerical experiment is the recovery of an arbitrary object, we selected the spoke target for the simulations. Note that the target contains information of a very wide range of spatial frequencies. To avoid undersampling problems in the central zone of the target due to the pixelated structure of digitized images, we used a modified version of it in which the central zone was removed. For our calculations we assumed a typical InI setup, that is, $f = 5.0$ mm, $p = \phi = 1.0$ mm, and $a = 100$ mm. In the simulation, four targets were placed at axial distances $z_1 = -75$ mm, $z_2 = -9.5$ mm, $z_3 = +8.0$ mm, $z_4 = +30$ mm as depicted in Fig. 2. Note that the axial positions are not symmetric about the reference plane, but correspond to the same amount of defocus as defined in terms of the well-known defocus coefficient $\omega_{20} = z\phi^2/2\lambda a(a-z)$ [17]. The elemental images are calculated according to (6), where the shot noise was simulated as

$$n_{\mathrm{SHOT}}^{\mathbf{m}}(\mathbf{x}') = \beta\sqrt{I_\lambda^{\mathbf{m}}(\mathbf{x}')}n_W(\mathbf{x}'). \tag{7}$$

Here β is a parameter that modifies the noise power and $n_W(\mathbf{x}')$ stands for Gaussian white noise of zero mean, and unity standard deviation. In the simulation we set $\beta = 0.13$, because it leads to a signal-to-noise ratio (SNR) of 40 dB. The images captured from nine different views are shown in Fig. 3, where we also show an enlarged image of the central element $\mathbf{m} = (0, 0)$. It is clear from the figure that the images of the spoke targets in z_1 and z_4 are highly blurred so that they cannot be recognized.

The easiest way for reducing the blurring would be reducing the numerical aperture of the microlenses. However, such an improvement is accompanied by a proportional deterioration of lateral resolution. This problem can be overcome by use of amplitude-modulation techniques. Specifically we propose the use of binary amplitude modulators. Such kind of modulators have been successfully applied to improve the performance of other 3-D imaging techniques such as confocal microscopy [23] or multiphoton scanning microscopy [24]. The technique consists in obscuring the central part of each microlens. Such an obscuration allows the secondary Huygens wavelets proceeding from the outer part of the lenses to interfere constructively in an enlarged axial range. Then by simply placing an opaque circular mask of diameter $D = \delta\phi$ (with $0 < \delta < 1$) just behind each microlens, one can increase the DOF of the microlens array. It is known that the higher the value of the obscuration ratio δ, the broader the axial intensity spot. In an ideal case one could obtain infinite depth of focus by approaching the value of δ to the unity. However, such a situation is not convenient from an experimental point of view, because the higher the value of δ the smaller the light efficiency of the system. On the other hand, if one works with only the outermost part of the lenses, the optical aberrations of the system dramatically increase. For these reasons, we propose to use the binary modulator of obscuration ratio $\delta = \sqrt{2}/2$. This modulator has a light efficiency of 50%, and doubles the DOF of the system (see Fig. 4). Thus we find that the impulse responses given by (3) remain practically invariant over a wide range of values of z. In other words, the use of amplitude-modulated microlenses permits to consider, in quite good approximation that the system is LSI over a wide

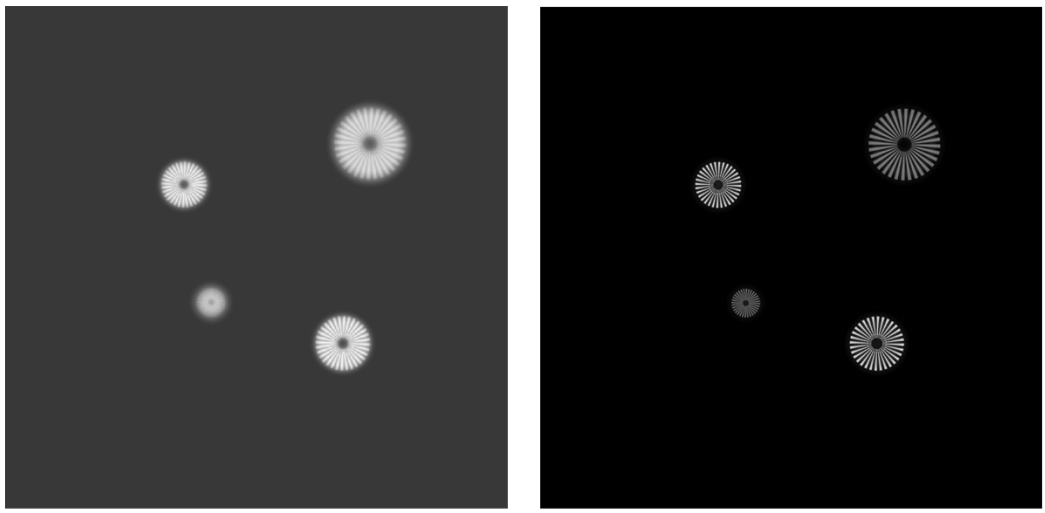

(a) (b)

Fig. 5. (a) Enlarged view of the central elemental image captured with the amplitude-modulated microlenses. (b) Same elemental image but processed by Wiener filtering.

range of axial distances and therefore, to define an effective PSF, which will be named as $H_{\text{eff}}(\mathbf{x})$.

IV. Deconvolution Tools: The Wiener Filtering

In real 2-D image acquisition tasks, the recorded signal, $i(\mathbf{x})$, depends not only on the convolution between the input signal and the PSF, but also on the noise signal. In mathematical terms,

$$i(\mathbf{x}) = s(\mathbf{x}) \otimes h(\mathbf{x}) + n(\mathbf{x}) \tag{8}$$

In this equation, $s(\mathbf{x})$ represents the input signal, $h(\mathbf{x})$ stands for the PSF, and $n(\mathbf{x})$ accounts for any type of additive noise. To recover the input signal from the output, one should perform a deconvolution operation. There are two general types of deconvolution methods: linear and nonlinear methods. The latter are more accurate, but they are all iterative methods. Since real-time processing is required in InI for a high number of elemental images, a low-time-consuming noniterative method is mandatory.

The optimal linear method for the signal recovery problem is the Wiener filtering [18]. The Wiener filter is given by

$$W(\mathbf{u}) = \frac{\tilde{h}^*(\mathbf{u})|\tilde{s}(\mathbf{u})|^2}{|\tilde{h}(\mathbf{u})|^2|\tilde{s}(\mathbf{u})|^2 + |\tilde{n}(\mathbf{u})|^2} \tag{9}$$

where symbol $\tilde{s}(\mathbf{u})$ stands for the Fourier transform of $s(\mathbf{x})$ and * denotes complex conjugation. Since $s(\mathbf{x})$, and therefore $\tilde{s}(\mathbf{u})$, is unknown, the filter cannot be used to recover the image. However, if we assume that we deal with white noise and a constant spectrum for the object, this expression can be approximated to

$$W(\mathbf{u}) = \frac{\tilde{h}^*(\mathbf{u})}{|\tilde{h}(\mathbf{u})|^2 + c\varphi^2} \tag{10}$$

where φ^2 can be understood as the noise-to-signal ratio in the frequency domain (NSRf) and the parameter $c \in \mathcal{R}^+$ controls the strength of the filtering. This filter is applied to the spectrum of the recorded signal

$$\tilde{\sigma}(\mathbf{u}) = \tilde{i}(\mathbf{u})W(\mathbf{u}) \tag{11}$$

and the recovery function $\sigma(\mathbf{x})$ is finally obtained by performing an inverse 2-D Fourier transform of (11).

In the previous section we showed that by the use of the amplitude-modulated microlenses the InI systems can be considered LSI in a neighborhood of the in-focus plane. Then Wiener filtering can be applied to recover the elemental images by using the effective PSF. After a thorough study of the method, we selected as $H_{\text{eff}}(\mathbf{x})$ the impulse response provided by an object point placed at $z_{\text{mid}} = +23$ mm. This PSF can be easily obtained by experimental measurement of the defocused spot produced by one microlens. The deconvolution procedure is performed by using this measured PSF [19]. Strictly speaking, only objects placed at this distance will be exactly recovered. Objects placed at other axial positions will be recovered quite approximately.

The value of φ^2 is usually obtained for any particular image after a trial-and-error process. However, due to the huge number of elemental images in an InI experiment, the development of a procedure for automatic application of deconvolution filtering is required. On the basis of an industrial standard of the National Electrical Manufacturers Association (NEMA) for the estimation of the SNR in diagnostic magnetic resonance, we have developed a new method to estimate the value of φ^2 in the Wiener filter. In this standard two exposures of the same object taken at two different times, $i_1(\mathbf{x})$ and $i_2(\mathbf{x})$, are needed for the calculations. According to this standard, the NSRf can be calculated by the following two different formulas:

$$\varphi_1^2 = \frac{1}{2}\min\left[\frac{|\tilde{i}_1(\mathbf{u}) - \tilde{i}_2(\mathbf{u})|}{|\tilde{i}_1(\mathbf{u})|}\right]^2 \tag{12}$$

and

$$\varphi_2^2 = \frac{1}{2}\frac{\langle|\tilde{i}_1(\mathbf{u}) - \tilde{i}_2(\mathbf{u})|^2\rangle}{\max[|\tilde{i}_1(\mathbf{u})|^2]} \tag{13}$$

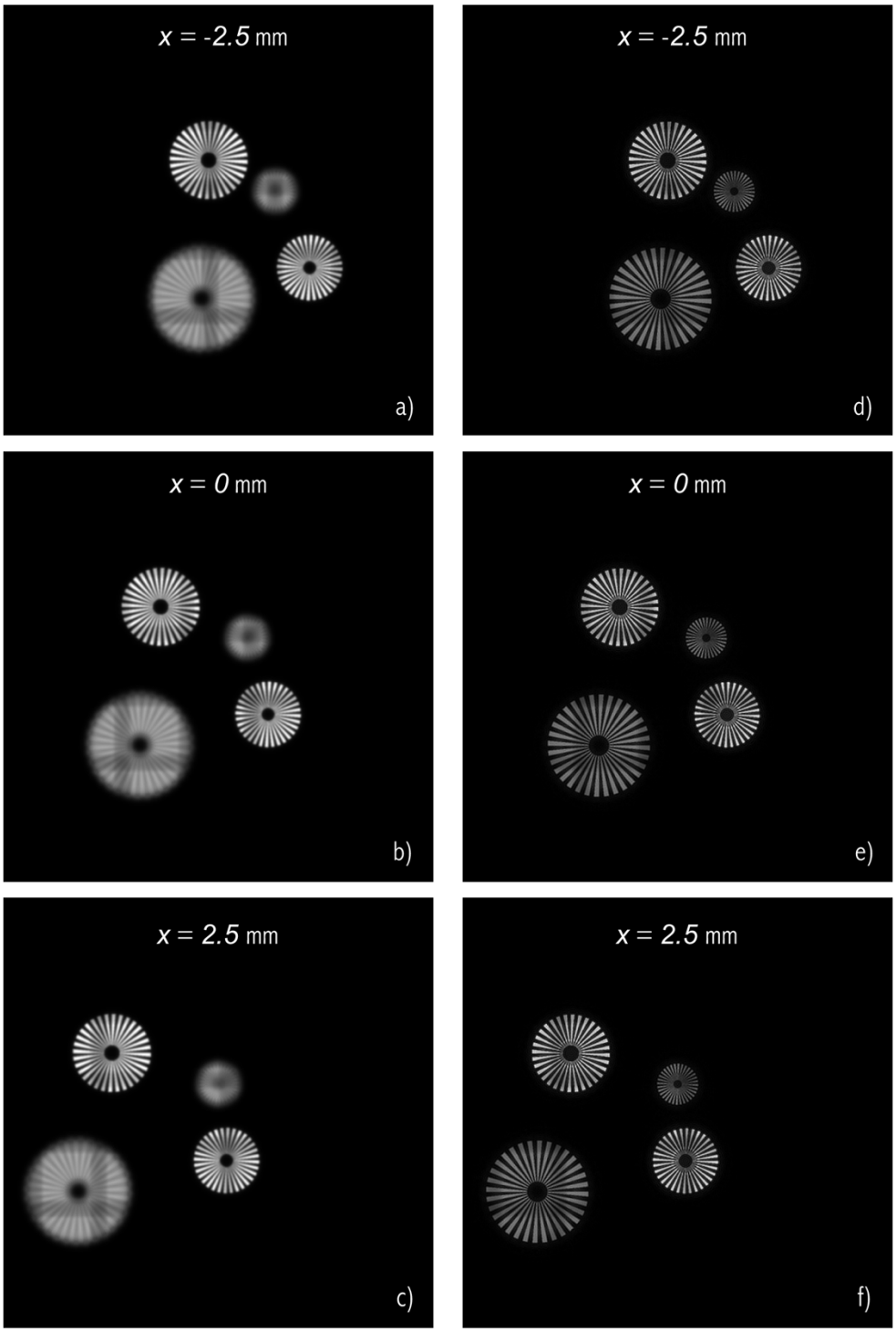

Fig. 6. Reconstructed image as seen by the observer from three different lateral positions. The central pictures correspond to the case in which the observer's eye is placed in front of the central microlens ($\mathbf{x} = 0$). The series of pictures correspond to: (a)–(c) The case in which neither the amplitude modulation nor the Wiener filtering were applied in capture procedure; (d)–(f) The case in which both techniques were applied. The value of lateral coordinate x refers to the lateral position of the observer as referred to the optical axis of the central microlens.

where

$$\langle f(\mathbf{x})\rangle = \frac{1}{N^2}\sum_{\mathbf{x}} f(\mathbf{x}) \tag{14}$$

is the mean value of $f(\mathbf{x}), N \times N$ being the number of pixels. Both formulas estimate the noise by means of the comparison between two consecutive images. We have found that (12) provides better results in images with high contrast (like text or even the spoke targets used in the previous chapter). However, (13) applies better when the image is of low contrast. So we use the mean value, namely

$$\varphi^2 = \frac{\varphi_1^2 + \varphi_2^2}{2} \tag{15}$$

as the best value for an automatic calculation. Concerning the value of parameter c in (10), it is noticeable that setting $c = 1$ gives the minimum mean-squared error reconstruction, while smaller values give reconstructions with sharpened edges at the expense of decreasing the signal-to-noise ratio (SNR) of the reconstruction [20]. Thus, we set $c = 0.1$ in our deconvolution calculations.

To illustrate the utility of our method, we have performed a numerical experiment. In the simulation we used the same pickup architecture shown in Fig. 2, but considering that the microlenses are amplitude modulated. Then we have applied the above-described deconvolution procedure to the acquired elemental images. The recovered elemental images are shown in Fig. 5. After comparing these images with those in Fig. 3, it is apparent that now the high-frequency information has been accurately recovered even for the most defocused planes.

To make our numerical experiment more visual, we have simulated in Fig. 6 the display process. In our calculations we assume an observer that is placed at a distance $D = 300$ mm from the microlens array and sees the reconstructed virtual orthoscopic image. We have calculated the observed image for three different lateral positions of the observer $x = -0.25$ mm, $0, +0.25$ mm, so that we can visualize the changes in perspective produced when the observer's eye is displaced parallel to the microlens array. The square grid in the pictures is due to the typical facetted structure of observed reconstructed integral images [21]. This figure, together with Fig. 5, shows that the proposed method provides a very efficient extension of DOF in InI.

V. Conclusion

We have proposed a new method to significantly extend the DOF for 3-D image pick-up in InI. In our two-step method we first proposed the insertion of a binary amplitude modulator, which alters the system's impulse response to have certain invariances over a wide range of axial distances. This fact allowed us to define an effective PSF which, otherwise, could not be defined. In the second step we adapted the Wiener deconvolution procedure to the InI sensor. After applying the deconvolution tool, we have obtained elemental images in which the DOF has been spectacularly extended. We have illustrated our method with a numerical experiment in which we have recovered the high-frequency information of a synthetic object even for the most defocused planes. The proposed method has broad applications in 3-DTV, 3-D display, and 3-D recognition [22].

References

[1] M. G. Lippmann, "Epreuves reversibles donnant la sensation du relief," *J. Phys. (Paris)*, vol. 7, pp. 821–825, 1908.

[2] H. E. Ives, "Optical properties of a Lippmann lenticulated sheet," *J. Opt. Soc. Amer.*, vol. 21, pp. 171–176, 1931.

[3] C. B. Burckhardt, "Optimum parameters and resolution limitation of integral photography," *J. Opt. Soc. Amer.*, vol. 58, pp. 71–76, 1968.

[4] T. Okoshi, "Optimum design and depth resolution of lens-sheet and projection type three-dimensional displays," *Appl. Opt.*, vol. 10, pp. 2284–2291, 1971.

[5] B. Javidi and F. Okano, *Three-Dimensional Television, Video, and Display Technology*. Berlin, Germany: Springer-Verlag, 2002.

[6] N. Davies, M. McCormick, and M. Brewin, "Design and analysis of an image transfer system using microlens arrays," *Opt. Eng.*, vol. 33, pp. 3624–3633, 1994.

[7] F. Okano, H. Hoshino, J. Arai, and I. Yayuma, "Real time pickup method for a three-dimensional image based on integral photography," *Appl. Opt.*, vol. 36, pp. 1598–1603, 1997.

[8] J. Arai, F. Okano, H. Hoshino, and I. Yuyama, "Gradient-index lens-array method based on real-time integral photography for three-dimensional images," *Appl. Opt.*, vol. 37, pp. 2034–2045, 1998.

[9] L. Erdmann and K. J. Gabriel, "High resolution digital photography by use of a scanning microlens array," *Appl. Opt.*, vol. 40, pp. 5592–5599, 2001.

[10] S. Kishk and B. Javidi, "Improved resolution 3D object sensing and recognition using time multiplexed computational integral imaging," *Opt. Exp.*, vol. 11, pp. 3528–3541, 2003.

[11] R. Martínez-Cuenca, G. Saavedra, M. Martínez-Corral, and B. Javidi, "Enhanced depth of field integral imaging with sensor resolution constraints," *Opt. Exp.*, vol. 12, pp. 5237–5242, 2004.

[12] J. S. Jang and B. Javidi, "Three-dimensional synthetic aperture integral imaging," *Opt. Lett.*, vol. 27, pp. 1144–1146, 2002.

[13] ——, "Improved viewing resolution of three-dimensional integral imaging by use of nonstationary micro-optics," *Opt. Lett.*, vol. 27, pp. 324–326, 2002.

[14] J. H. Park, S. Jung, H. Choi, and B. Lee, "Integral imaging with multiple image planes using uniaxial crystal plate," *Opt. Exp.*, vol. 11, pp. 1862–1875, 2003.

[15] J.-S. Jang and B. Javidi, "Large depth-of-focus time-multiplexed three-dimensional integral imaging by use of lenslets with nonuniform focal lengths and aperture sizes," *Opt. Lett.*, vol. 28, pp. 1924–1926, 2003.

[16] M. Martínez-Corral, B. Javidi, R. Martínez-Cuenca, and G. Saavedra, "Integral imaging with improved depth of field by use of amplitude modulated microlens array," *Appl. Opt.*, vol. 43, pp. 5806–5813, 2004.

[17] A. Stokseth, "Properties of a defocused optical system," *J. Opt. Soc. Amer.*, vol. 59, pp. 1314–1321, 1969.

[18] C. W. Helstrom, "Image restoration by the method of least squares," *J. Opt. Soc. Amer.*, vol. 57, pp. 297–303, 1967.

[19] X. Lai, Z. Lin, E. S. Ward, and R. J. Ober, "Noise suppression of point spread functions and its influence on deconvolution of three-dimensional fluorescence microscopy image sets," *J. Micros.*, vol. 217, pp. 93–108, 2005.

[20] J. R. Fienup, D. Griffith, L. Harrington, A. M. Kowalczyk, J. J. Miller, and J. A. Mooney, "Comparison of reconstruction algorithms for images from sparse-aperture systems," in *Proc. SPIE 4792*, 2002, pp. 1–8.

[21] M. Martínez-Corral, B. Javidi, R. Martínez-Cuenca, and G. Saavedra, "Multifacet structure of observed reconstructed integral images," *J. Opt. Soc. Amer.*, vol. 22, pp. 597–603, 2005.

[22] Y. Frauel, E. Tajahuerce, O. Matoba, A. Castro, and B. Javidi, "Comparison of passive ranging integral imaging and active imaging digital holography for three-dimensional object recognition," *Appl. Opt.*, vol. 43, pp. 452–462, 2004.

[23] C. J. R. Sheppard, "Binary optics and confocal imaging," *Opt. Lett.*, pp. 505–506, 1999.

[24] M. Martínez-Corral, C. Ibáñez-López, G. Saavedra, and M. T. Caballero, "Axial gain resolution in optical sectioning fluorescence microscopy by shaded-ring filters," *Opt. Exp.*, vol. 11, pp. 1740–1745, 2003.

Raul Martínez-Cuenca received the B.Sc. in photonics and M.Sc. degrees in physics from the University of Valencia, Valencia, Spain, in 2003 and 2005, respectively, where he is currently a Research Student of Optics.

Since 2003 he has been working with the "3D Diffraction and Imaging Group", at the Optics Department, University of Valencia, Spain. His research interest includes focusing properties of light, and 3-D imaging acquisition and display. He has published on these topics five publications subject to peer review.

Genaro Saavedra, photograph and biography not available at time of publication.

Manuel Martínez-Corral received the M.Sc. and Ph.D. degrees from the same University in 1988 and 1993, respectively.

He is currently a Professor of Optics at the University of Valencia. Since 1999 he has led the "3D Diffraction and Imaging Group", at the Optics Department. His research interest includes focusing properties of light, point-spread-function engineering in 3-D microscopy, and 3-D imaging acquisition and display. He has published on these topics more than 50 publications subject to peer review.

Bahram Javidi (M'80–SM'93–F'98) received the B.S. degree in electrical engineering from George Washington University, Washing, DC, in 1980, and the M.S. and Ph.D. degrees in electrical engineering from Pennsylvania State University, Philadelphia, in 1982 and 1986, respectively.

He is the Board of Trustees Distinguished Professor at the University of Connecticut, Storrs. He has held visiting positions during his sabbatical leave at Massachusetts Institute of Technology, U.S. Air Force Rome Laboratory at Hanscom Base, and at Thomson-CSF Research Laboratories in Orsay, France. He has completed several books including *Optical and Digital Techniques For Information Security* (Springer, 2004), *Three Dimensional Television, Video, and Display Technologies* (Springer Verlag, 2002), *Smart Imaging Systems* (SPIE Press, 2001). He has published over 160 technical articles in major journals. He has published over 200 conference proceedings, including over 60 invited conference papers, and 60 invited presentations. His research interests are the areas of digital image processing, three dimensional display, three dimensional signal processing, biomedical image processing, pattern recognition, 3-D neural networks, secure information systems, and optical data storage.

Dr. Javidi is a Fellow of the Optical Society of America (OSA), and a Fellow of the International Society for Optical Engineering (SPIE). He has received the IEEE Lasers and Electro-Optics Society Distinguished Lecturer Award in 2003. He was the recipient of the IEEE Best Journal Paper Award from IEEE TRANSACTIONS ON VEHICULAR TECHNOLOGY in 2002. He has served as the Chairman of the IEEE Lasers and Electro-Optics (LEOS) Technical Committee on Electro-optics Sensors and Systems, and a member of the IEEE Neural Networks Council.